Ex vivo expansion of murine MSC impairs transcription factor induced differentiation into pancreatic β-cells

Dario Gerace (PhD)[1], Rosetta Martiniello-Wilks (PhD)[1, 2], Rosaline Habib (PhD)[1], Binhai Ren (PhD)[1], Najah Therese Nassif (PhD)[1], Bronwyn Anne O'Brien (PhD)[1] and Ann Margaret Simpson (PhD)[1]

[1]The School of Life Sciences and Centre for Health Technologies, Faculty of Science, University of Technology Sydney, Sydney, Australia

[2]Translational Cancer Research Group, University of Technology Sydney, Sydney, Australia

Running title: Gene and adult stem cell therapy for T1D

Address correspondence to: Prof. Ann M. Simpson

School of Life Sciences

University of Technology Sydney

15 Broadway, Ultimo, NSW, 2007, Australia

Ann.Simpson@uts.edu.au

Word Count: 4811

Keywords: diabetes, differentiation, gene therapy, insulin secretion, stem cell

Footnote: Dr Dario Gerace's current affiliation: Department of Stem Cell and Regenerative Biology, Harvard Stem Cell Institute, Harvard University, Cambridge, MA, USA.

Abstract

Combinatorial gene and cell therapy as a means of generating surrogate β-cells has been investigated for the treatment of type 1 diabetes (T1D) for a number of years with varying success. One of the limitations of current cell therapies for T1D is the inability to generate sufficient quantities of functional, transplantable insulin-producing cells. Due to their impressive immunomodulatory properties, in addition to their ease of expansion and genetic modification *ex vivo*, mesenchymal stem cells (MSC) are an attractive alternative source of adult stem cells for regenerative medicine. To overcome the aforementioned limitation of current therapies, we assessed the utility of *ex vivo* expanded bone-marrow derived murine MSCs for their persistence in immune-competent and immune-deficient animal models, and their ability to differentiate into surrogate β-cells.

$CD45^-/Ly6^+$ murine MSCs were isolated from the bone marrow of non-obese diabetic (NOD) mice and nucleofected to express the bioluminescent protein, *Firefly luciferase (Luc2)*. The persistence of a subcutaneous (s.c) transplant of *Luc2*-expressing MSCs was assessed in immune-competent (NOD) (n=4) and immune-deficient (NOD/*Scid*) (n=4) animal models of diabetes. *Luc2*-expressing MSCs persisted for 2 and 12 weeks, respectively, in NOD and NOD/*Scid* mice. *Ex vivo* expanded MSCs were transduced with the HMD lentiviral vector (MOI=10) to express furin-cleavable human insulin (*INS-FUR*) and murine *NeuroD1* and *Pdx1*. This was followed by the characterization of pancreatic transdifferentiation via reverse transcriptase polymerase chain reaction (RT-PCR), and static and glucose stimulated insulin secretion (GSIS). *INS-FUR*-expressing MSCs were assessed for their ability to reverse diabetes after transplantation into streptozotocin (STZ)-diabetic NOD/*Scid* mice (n=5). Transduced MSCs did not undergo pancreatic transdifferentiation, as determined by RT-PCR analyses, lacked glucose-responsiveness, and upon transplantation did not reverse diabetes.

The data suggests that *ex vivo* expanded MSCs lose their multipotent differentiation potential and may be more useful as gene therapy targets prior to expansion.

Keywords

Mesenchymal stem cells, Type 1 diabetes, Lentivirus, Bioluminescence imaging, Differentiation, Insulin-producing cells

Introduction

T1D results from the autoimmune destruction of the pancreatic insulin-producing β-cells, which leads to hyperglycaemia and the lifelong dependence on exogenous insulin therapy[1]. Currently, the only cures for T1D are pancreas or islet transplantation, however these interventions are limited by a shortage of donor organs and the requirement for lifelong immunosuppression[2]. To overcome the limitations of current therapies, a promising alternative strategy is the *ex vivo* generation of surrogate β-cells through the directed-differentiation of non-pancreatic target cells[3-10].

Pancreatic transcription factors play an important role both in islet cell differentiation and specialisation, and mature β-cell function during embryonic and neonatal development and adult life, respectively[11, 12]. Our laboratory, and others, have investigated the direct transfer of β-cell transcription factors and insulin as mediators of pancreatic transdifferentiation in non-pancreatic cells/tissues with varying success[3-5, 13-17]. We have previously shown that the endocrine specifying transcription factor, *NeuroD1*, which lies downstream of *Pdx1* in the transcription factor hierarchy of pancreatic development, was capable of inducing pancreatic transdifferentiation of a rat hepatocyte cell line (H4IIE). Transdifferentiation was characterized by the upregulation of both upper and lower-hierarchy pancreatic transcription factors, without the development of exocrine differentiation[12, 18]. In addition, due to the over-expression of the

62 furin-cleavable human insulin (*INS-FUR*) gene (a modified form of human pro-insulin, which permits
63 cleavage into mature insulin via furin enzymes in non-pancreatic cells), these cells were capable of
64 synthesizing, storing and secreting mature human insulin in a glucose-responsive manner; and reversed
65 diabetes upon transplantation in STZ-diabetic NOD/*Scid* mice[18]. However, one of the current challenges
66 of clinical translation of combinatorial gene and cell therapies for T1D is upscaling the production of
67 functional surrogate β-cells[19].

68 Due to their high plasticity, immunomodulatory properties, fewer ethical concerns, and ease of *ex vivo*
69 expansion and gene modification[20, 21], MSCs are an attractive alternative target cell for the autologous and
70 allogeneic treatment of T1D. Several studies have investigated the *ex vivo* targeting of MSCs for
71 transdifferentiation into islet progenitor cells (IPCs) via viral-mediated transfer of pancreatic transcription
72 factors[14-17]. Previously, the transfer of the "master regulator" of pancreatic differentiation, *Pdx1*, to MSCs
73 resulted in their differentiation into glucose-responsive IPCs, which reversed diabetes, for a period of 6-8
74 weeks (experimental endpoint), upon transplantation into STZ-diabetic NOD/*Scid* mice[14]. However, *Pdx1*
75 transfer has also been associated with exocrine differentiation, and concomitant tissue damage, which is
76 undesirable for a T1D cell replacement therapy[22]. Therefore, in this study, we assessed the pancreatic
77 differentiation potential of *ex vivo* expanded murine bone-marrow derived MSCs as a pre-clinical model
78 to overcome the shortage limitations of current therapies, via the over-expression of murine *NueroD1*
79 and *INS-FUR* using a lentiviral vector. We found that due to a loss of the intrinsic multipotent
80 differentiation potential of MSCs with increasing culture, transcription factor mediated β-cell
81 differentiation, via the forced expression of *NeuroD1* and *INS-FUR*, failed to occur. This was confirmed via
82 the over-expression of murine *Pdx1*, which is known to induce β-cell differentiation of MSCs at early
83 passage numbers. The data highlights the limited timeframe for MSCs to function as effective gene
84 therapy targets, and suggests that MSCs do not represent a suitable alternative source of cells to
85 overcome the shortage limitations of current β-cell replacement therapies.

Methods

Sourcing of animals

NOD and NOD/*Scid* mice were sourced from the Animal Resources Centre (WA, Australia). All animal work was approved by the UTS Animal Care and Ethics Committee (ACEC 2011-447A; ACEC 2009-244A), and complied with the Australian code for the care and use of animals for scientific purposes[23].

MSC isolation and cell culture

Bone marrow was flushed from the femurs of female NOD mice (6-8 weeks old), and the cell pellet was resuspended in standard MSC medium (α-minimal essential media [MEM], 1% v/v 100x Penicillin/Streptomycin/L-Glutamine (P/S/G) with 20% v/v Fetal Bovine Serum [FBS]) (Gibco®, Thermofisher), and incubated at 37°C/5% CO_2. Plastic-adherent stromal cells were sub-cultured for two passages (with epiphyses) prior to fluorescence-activated cell sorting (FACS).

Passage 2 plastic-adherent stromal cells ($5x10^5$ cells) were resuspended in sorting buffer (1x Hanks Balanced Salt Solution [HBSS] supplemented with 5% v/v FBS) and stained with 0.2mg/ml rat anti-mouse CD45 monoclonal antibody (mAb) conjugated to allophycocyanin (APC) (BD Pharmingen™, USA) and 0.2mg/ml rat anti-mouse Ly6 (Sca-1) mAb conjugated to phycoerythrin (PE) (BD Pharmingen™, USA). Stained stromal cells were sorted by FACS at the Advanced Cytometry Facility (Centenary Institute, Sydney, Australia) using a BD FACSAria™ II flow cytometer, and analysed using BD FACSDiva™ software (Version 6.1.3). The stromal cells were sorted into $CD45^-/Ly6^+$ (MSCs) and $CD45^+/Ly6^+$ (double positive) cell populations. Sorted cells were resuspended in complete medium and incubated at 37°C/5% CO_2. Following cell attachment, 10ng/ml basic fibroblast growth factor (bFGF) was added to the standard MSC medium, in which the parental stromal cells and sorted cells were cultured thereafter.

MSC proliferation and clonogenicity

For proliferation assays, MSCs at early (P3-15), mid (P15-30), and late (P30-60) passage number were seeded in 24-well plates ($2.5x10^3$ cells/well) (Falcon® BD Biosciences, San Jose, USA) in triplicate, and maintained in standard MSC medium for 15 days, with medium replenished weekly. Cell viability was assessed by Trypan Blue (0.4% v/v; Gibco®, Thermofisher) exclusion. Total cell and viable cell numbers were determined, and represented as mean ± standard deviation (SD) for each time point (n=3).

For clonogenicity assays, MSCs at early, mid and late passage number were seeded in $10cm^2$ tissue culture treated plates ($5x10^2$ cells/plate) (Falcon® BD Biosciences), and maintained in standard MSC medium for 10 days. Colonies were stained with 0.4% v/v methylene blue in methanol, and counted by microscopy. Data were represented as mean colony count per 5000 cells ± SD (n=3). Standard MSC medium was replenished weekly.

Morphological analysis

Images of four fields of view at 10x or 20x magnification were acquired at early, mid and late passage number using a Leica© DM microscope (Leica Microsystems©, Weltzar, Germany), and processed using the image processing software, Leica Application Suite (V4.4.0) (Leica Microsystems©). Scale bars on figures are equivalent to 100µm.

Gene expression profiling

Total RNA was extracted using TRIzol® Reagent (Thermofisher®, Waltman, USA) and samples were treated with DNase I, Amplification Grade (Thermofisher®, USA) before cDNA synthesis using SuperScript® III First-Strand Synthesis SuperMix (Thermofisher®, USA). RT-PCR was subsequently performed using an Eppendorf® Mastercycler (Eppendorf™, Hamburg, Germany) to determine the relative expression levels of

selected pancreatic genes using GoTaq PCR Mastermix (Promega®, Madison, USA), and the previously published oligonucleotide sequences and optimised PCR protocols **(Supplementary Table 1)**[4]. PCR products were imaged after electrophoresis on a 1% w/v agarose gel stained with 10000x GelRed™ (Biotium®, Fremont, USA) (1:100000) on the InGenius3 (Syngene®, Frederick, USA) UV transilluminator using the GeneSys image acquisition software (Syngene®).

Differentiation assays

Adipogenesis

Early, mid and late passage number cells were seeded in standard MSC medium in 24-well plates ($2.5x10^4$ cells/well) in triplicate and grown to 80-90% confluency. The medium was subsequently replenished with either adipogenic control or differentiation medium, as previously described[24]. The cells were stained with 0.2% w/v Oil Red O in methanol (Fronine®, Sydney, Australia), and semi-quantitatively scored as previously described [24]. Values were expressed as count per cm^2 and were represented as means ± SDs (n=3).

Osteogenesis

Early, mid and late passage cells were seeded in standard MSC medium in 24-well plates ($1.25x10^4$ cells/well) in triplicate and grown to 90-95% confluence. The medium was subsequently replenished with either osteogenic control or differentiation medium, as previously described[24]. The cells were stained with 2% w/v Alizarin Red S (pH 4.1) (Fronine®) and semi-quantitatively scored, as previously described[24]. Values were expressed as count per cm^2 and were represented as means ± SDs (n=3).

Chondrogenesis

Early, mid and late passage cells were seeded in 24-well plates ($1.25x10^4$ cells/well) and grown to 90% confluence in standard MSC medium. The medium was subsequently replenished with either control (MesenCult™-ACF Chondrogenic Differentiation Basal Medium [STEMCELL Technologies®, Vancouver, Canada] with 2mM L-glutamine) or differentiation (MesenCult™-ACF Chondrogenic Differentiation Basal Medium, 2mM L-glutamine, MesenCult™-ACF 20X Chondrogenic Differentiation Supplement) medium, and incubated at 37°C/5% CO_2 for 18 days. On day 18, the cells were fixed in 10% v/v neutral buffered formalin and stained with Alcian blue solution (8x, pH2.5) (Sigma-Aldrich™, Sydney, Australia). Chondrogenesis was visualised by Alcian blue staining of filamentous glycosaminoglycans.

Construction of mammalian plasmid pVITRO-*Luc2*

The manipulation of genetic material and generation of genetically modified organisms was approved by the UTS Biosafety Committee (2001-19-R-GC; 2009-02-R-GC). The luciferase reporter gene *Luc2* (*Photinus pyralis*), encoded within the vector pGL4.20 (*Luc2*/Puro) (Promega®, Ipswich, USA) was digested with the restriction enzymes, EcoRV-HF® and BamHI-HF® (New England Biolabs®, San Diego, USA), and ligated into the mammalian dual expression plasmid pVITRO2-hygro®-mcs (InvivoGen®, San Diego, USA), to generate the mammalian bioluminescence plasmid pVITRO2-*Luc2* (**Supplementary Fig. 1a**).

Nucleofection

Early passage MSCs ($1x10^6$ cells) were nucleofected with 5µg pVITRO2-*Luc2* and 2µg pmax-GFP®, according to the manufacturer's instructions (Lonza™, Basel, Switzerland), using the Nucleofector™ 2b device (Lonza™). Following nucleofection, the cells were returned to culture in standard MSC medium at 37°C/5% CO_2 for one week. Stable clones were then selected using 200µg/ml Hygromycin B (Thermofisher Scientific®) over a two-week period.

***In vitro* bioluminescence imaging (BLI)**

In vitro BLI of a linear concentration of mid-passage MSC-*Luc2*, and the cell line MSC-*Luc2/LacZ ID7* (positive control), was performed in 96-well ViewPlate microplates (PerkinElmer®, Waltman, USA). Cells were attached overnight and imaged on the IVIS Lumina II (PerkinElmer®) following the addition of 150µg/ml D-Luciferin (Gold Biotechnology®, St. Louis, USA). For quantification, a region of interest (ROI) was manually selected using the Living Image (Version 3.1) software. BLI intensity values were represented as the mean average radiance ± SD (p/s/cm^2/sr).

In vivo MSC persistence

NOD (n=4) and NOD/*Scid* (n=4) mice (6-10 weeks of age), received a total of six subcutaneous (s.c.) injections of 1x10^4 (n=2), 1x10^5 (n=2) and 1x10^6 (n=2) mid-passage MSC-*Luc2* cells/mouse. Untreated age-matched NOD (n=2) and NOD/*Scid* (n=2) mice were utilized as negative controls. Mice were anaesthetised using 2.5% Isoflurane carried in O_2 (1.5L/min), transferred to the IVIS Lumina II imaging unit, and maintained under anaesthesia. BLI images were acquired 5 min after the intraperitoneal (i.p.) injection of D-luciferin (15mg/mL) at 150mg/kg or 10µL/g. For quantification, ROI were manually selected using the Living Image (Version 3.1) software. BLI intensity values were presented as the mean average radiance ± standard errors of means (SEMs) (p/s/cm^2/sr).

Construction of lentiviral plasmids

The pHMD and pHMD-*INS-FUR* lentiviral plasmids [3-5] were modified to express *INS-FUR* and the human codon-optimized murine (*Mus musculus*) *Neurod1* and *Pdx1* genes. Using GeneArt Gene Synthesis™ (Thermofisher®, USA), murine *Neurod1* cDNA (NM_010894) was synthesized linked to eGFP via a T2A peptide at the C-terminus. The *Neurod1-T2A-eGFP* sequence was PCR amplified using the forward and reverse primers, 5'-GATACTTGGCCATATGACCAAATCATACAGCGA-3' and 5'-CCATGAGGCCCAGTTAAT-3', containing MscI and the PacI restriction sites, respectively. PCR amplified *Neurod1-T2A-eGFP* was ligated

into pHMD and pHMD-*INS-FUR* following digestion with MscI and PacI (New England Biolabs®, Waltman, USA) to generate pHMD-*Neurod1* and pHMD-*Neurod1/INS-FUR*, respectively.

The pAAV-*Pdx1* plasmid (donated by Dr Grant Logan, Children's Medical Research Institute, Westmead Children's Hospital, Sydney, Australia) containing the murine *Pdx1* cDNA (NM_008814.3) and the fluorescent reporter mCherry upstream and downstream of the internal ribosomal entry site (IRES), respectively, was used to clone murine *Pdx1* into the HMD lentiviral plasmid. The *Pdx1-IRES-mCherry* sequence was PCR amplified using the forward and reverse primers, 5'-GATACTGGATCCATGAACAGCGAGGAACAG-3' and 5'-GCGCCGTTAATTAATTACTTGTACAGCTCGTC-3', containing BamHI and PacI restriction sites, respectively. PCR amplified *Pdx1-IRES-mCherry* was ligated into pHMD following digestion with BamHI-HF® and PacI (New England Biolabs®, USA) to generate pHMD-*Pdx1*. Schematic representations of the cloned lentiviral plasmids are illustrated in **Supplementary Fig. 1b**.

Lentiviral vector propagation and titration

Lentiviral plasmids were co-transfected into HEK293T cells using calcium phosphate precipitation as previously described[3-5]. Lentiviral particles were harvested at 36, 48, 60 and 72 hrs post-transfection, filtered through Millex-HV 0.45µM polyvinylidene fluoride syringe filters (EMD Millipore©, Burlington, USA), and concentrated using Amicon Ultra 100 kDa filters (EMD Millipore©, USA). Concentrated lentiviral particles were titered using NIH3T3 cells and FACS analysis of eGFP and mCherry expression. Flow cytometry data was analyzed using BD FACSDiva™ software (Version 8.0.1).

Viral transduction

Mid-passage MSC-*Luc2* ($1x10^5$ cells/well) were transduced overnight (MOI=10) with HMD, HMD-*INS-FUR*, HMD-*Neurod1*, HMD-*Neurod1/INS-FUR,* and HMD-*Pdx1* in standard MSC medium supplemented with

8µg/ml Polybrene (Sigma-Aldrich™, Australia). Following transduction, lentiviral particles were removed and the cells cultured for 72 hrs, after which the cells were sorted into $eGFP^+$ and $mCherry^+$ populations at the Advanced Cytometry Facility (Centenary Institute, Sydney, Australia) using a BD FACSAria™ II, and analysed using BD FACSDiva™ software (Version 6.1.3). Fluorescence imaging of positively transduced MSCs was performed using a Leica© DM microscope (Leica Microsystems©, Australia).

Chronic and acute insulin secretion

For chronic insulin secretion, untransduced and transduced MSCs ($1x10^5$ cells/well in triplicate, n=4) were cultured for 24 hrs in standard MSC medium. For glucose-stimulated insulin secretion, untransduced and transduced MSCs ($1x10^5$ cells/well in triplicate, n=3) were seeded in 6-well plates and sequentially stimulated with 20mM D-Glucose (Sigma-Aldrich™, Australia), as previously described[25]. The human insulin concentrations in harvested supernatants, from both chronic and acute insulin secretion assays, were quantified using the ARCHITECT™ i4000SR Immunoassay Analyser (Abbott Diagnostics®, Macquarie Park, Australia). Data were represented as mean insulin concentration (pmol/ml/$1x10^5$ cells) ± SD.

Induction of diabetes in NOD/*Scid* mice

NOD/*Scid* mice received 170mg/kg of STZ in 0.1M sodium citrate buffer (pH 4.0) via i.p. injection. All animals, including non-diabetic controls, had their body weights and blood glucose concentrations measured daily using an Accu-Chek® Performa glucometer (Accu-Chek®, Roche, Castle Hill, Australia). Animals that did not develop hyperglycaemia (blood glucose concentration >8mmol/L) within 1-week post STZ-injection received a second low dose (40mg/kg) STZ-injection. Animals that displayed hyperglycaemia for four consecutive days were considered diabetic and were used for *in vivo* experiments.

Transplantation of MSC in STZ-NOD/*Scid* mice

Two groups of STZ-diabetic NOD/*Scid* mice received s.c. injections of $1x10^7$ (n=6) and $5x10^7$ (n=6) late passage *INS-FUR*-expressing MSCs, respectively. Non-diabetic (n=6) and untreated diabetic (n=6) animals were assessed alongside treated animals. Body weights and blood glucose concentrations were measured daily. Animals that displayed hypoglycaemia (blood glucose concentration <3mmol/L) or body weight loss (>10%) for two consecutive days were euthanized by CO_2 asphyxiation and cervical dislocation.

Intraperitoneal glucose tolerance test (IPGTT)

Normal (n=5) and treated (n=3) mice were fasted for 6 hrs, transferred to a ZDS Qube Manifold 5 Station (Advanced Anesthesia Specialists®, Australia) and maintained under stable anaesthesia (2.5L/min isoflurane and 1.5L/min O_2). Mice received an i.p. injection of 2g/kg 50% v/v liquid glucose (0.5g/ml). Blood glucose was measured at 0, 5, 15, 30, 60, and 90 min post-injection. Following IPGTTs, animals were euthanized by CO_2 asphyxiation and cervical dislocation.

Statistical analysis

All statistical analysis was performed using GraphPad Prism 7® software. Values were presented as means ± SDs or SEMs. One-way or two-way ANOVAs, with the appropriate post-tests, were performed, with $p< 0.05$ indicating significance.

Results

***In vitro* characteristics of NOD MSCs**

MSCs identified by FACS were characterized by the surface marker profile $CD45^-/Ly6^+$, and constituted ~33% of the parental stromal cell population (**Fig. 1a**). MSCs displayed the characteristic fibroblast-like morphology from early to late passage number (**Fig. 1b**). However, a decrease in MSC diameter was

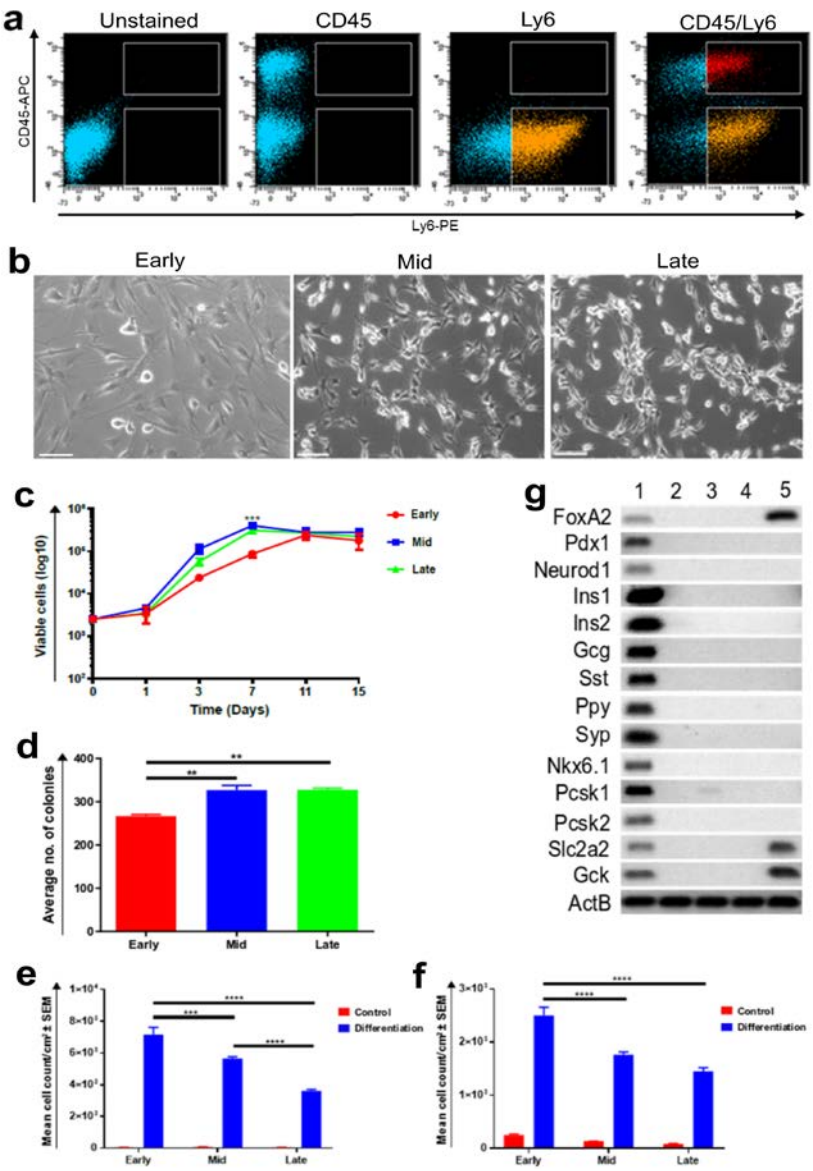

Figure 1: *In vitro* characteristics of NOD derived MSCs with cell culture expansion (a) FACS analysis and enrichment of NOD derived MSCs. Following culture for two passages, NOD bone marrow stromal cells were stained with nil antibody (Unstained), CD45 mAb conjugated to fluorochrome APC (CD45-APC), Ly6 MAb conjugated to fluorochrome PE (Ly6-PE) and both mAbs (CD45-APC/Ly6-PE). Fluorescence dot plots of CD45-APC (y-axis) and Ly6-PE (x-axis) were used to identify the MSC ($CD45^-/Ly6^+$; orange) and double positive ($CD45^+/Ly6^+$; red) cell subpopulations ready for cell sorting using the BD FACSAria™ II instrument. Representative of three individual FACS sorting experiments; (b) Plastic adherence, fibroblast-like morphology and self-renewal without differentiation into other cell types. MSCs maintained fibroblast-like morphology as assessed using light microscopy (Leica DM microscope; 10x magnification; scale bar = 100μM); (c) Improved cell proliferation with culture expansion. Data are presented as mean viable cells ± SDs (n=3). A two-way ANOVA with Tukey's post tests were performed, *p<0.05; (d) Improved fibroblastic colony formation following Methylene blue staining. Data are presented as mean number of colonies ± SEMs (n=3). A one-way ANOVA and Tukey's post tests were performed, * p<0.05; (e) Semi-quantitative analysis of adipogenic differentiation under defined conditions. NOD derived MSCs maintained fat formation following Oil Red O staining, albeit at reduced levels, with increasing passage number. Data are presented as mean cell count/cm^2 ± SEM (n=3). A two way ANOVA and Tukey's post tests were performed, * p<0.05; (f) Semi-quantitative analysis of osteogenic differentiation under defined conditions. NOD derived MSC maintained bone formation following Alizarin Red staining, albeit at lower levels, with increasing passage number. Data are presented as mean cell count/cm^2 SEM (n=3). A two way ANOVA and Tukey's post tests were performed, * p<0.05; (g) Pancreatic transcription factor, hormone and protein expression levels were determined by RT-PCR. MSCs did not express any transcription factors, hormones or protein found in the pancreas. Positive control mouse pancreas (Lane 1), plastic-adherent MSCs (Lane 2), plastic-adherent hematopoietic cells (Lane 3), adherent bone marrow cells (Lane 4), and negative control mouse liver (Lane 5).

observed with increasing passage, from ~100µm (early passage) to 50µm (late passage). Although MSCs underwent a period of early passage replicative crisis during P5-8 (data not shown), MSCs continued to self-renew up to 60 passages (maximum culture period). An intra-population analysis of MSC proliferation and clonogenicity showed no significant difference in proliferation (**Fig. 1c**) and conservation of clonogenicity potency (**Fig. 1d**) from early to late passage number.

To demonstrate that NOD MSCs underwent tri-lineage differentiation, as defined by the International Society Cell and Gene Therapy (ISCT), tri-lineage differentiation assays were performed at early, mid and late passage number. NOD MSC demonstrated tri-lineage differentiation into adipocytes (**Supplementary Fig. 2**), osteocytes (**Supplementary Fig. 3**), and chondrocytes (**Supplementary Fig. 4**). Semi-quantitative analysis of adipogenesis and osteogenesis was assessed by scoring the degree of differentiation, as previously described[24]. MSCs displayed reduced adipogenesis (**Fig. 1e)** and osteogenesis (**Fig. 1f**) with increasing passage number.

To confirm that MSCs did not intrinsically express any pancreatic transcription factors or hormones, RT-PCR analyses were performed, and showed a lack of expression of pancreatic transcription factors, hormones and proteins in all adherent bone marrow cell populations (**Fig. 1g)**. As expected, all genes were expressed in normal mouse pancreas (positive control), and *FoxA2*, *Scl2a2* and *Gck* were expressed in normal mouse liver (negative control).

Syngeneic MSCs are cleared in an immune-competent animal model

Non-invasive BLI is an established and sensitive tool for assessing cell replacement therapy safety and efficacy in living preclinical small animal models. Furthermore, preclinical BLI results often serve as the decision point of the suitability of a cell replacement therapy for clinical trial testing in humans. This study utilized the Firefly luciferase reporter gene, *Luc2*, a *Luc2* specific light producing substrate D-luciferin and

an IVIS Lumina II imaging system (Perkin Elmer©). Prior to performing *in vitro* and *in vivo* BLI, a clonal population of MSCs expressing *Luc2* (MSC-*Luc2*) was obtained by selection with Hygromycin B. MSC-*Luc2* retained a fibroblast-like morphology similar to that observed for parental MSCs (**Fig. 2a**), however these cells exhibited a reduced cell diameter (~100µm nucleofected versus 150µm parental). *In vitro* analyses of BLI at multiple time-points over a 3-hour period (**Fig. 2b**), in combination with linear regression analysis (**Fig. 2c**), confirmed that a clonal population of MSC-*Luc2* had been selected, and that bioluminescence was stable for up to 3 hrs *in vitro*.

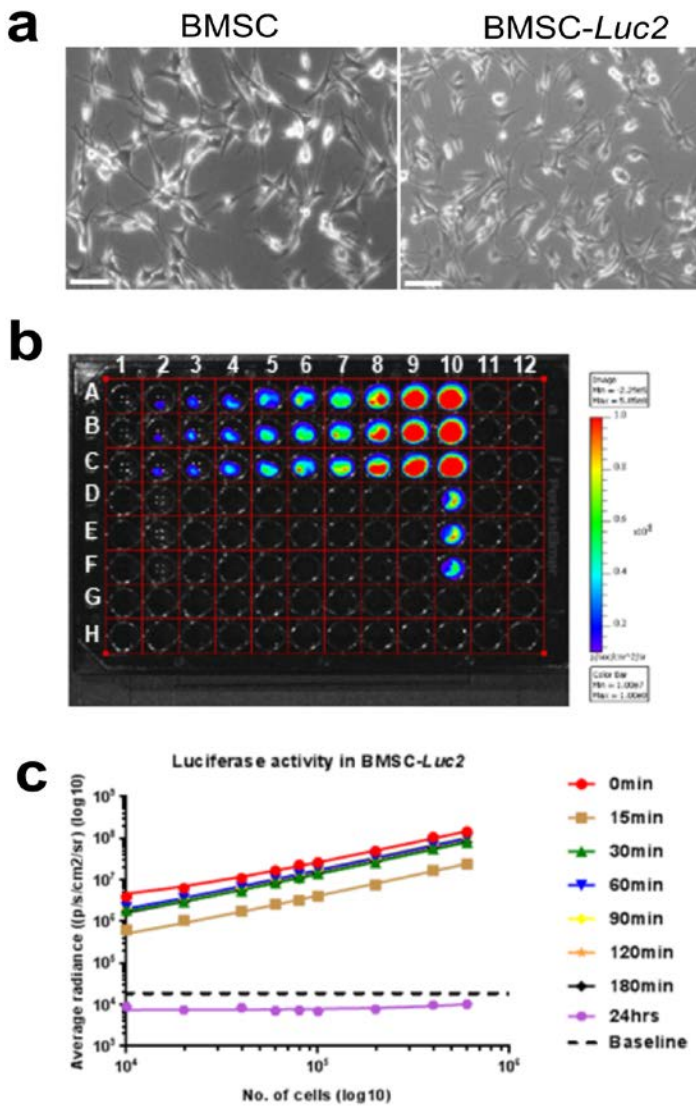

Figure 2: NOD derived MSC nucleofection (a) MSCs (early passage number) were nucleofected with 0 and 5µg pVITRO2-*Luc2*. Parental MSCs and MSC-*Luc2* at an equivalent passage number (P15) showed native fibroblast-like morphology and maintained plastic adherence and self-renewal properties. Images were acquired on a Leica DM light microscope at 10x magnification, scale bar = 100µm; (b) *In vitro* functional characterization of luciferase activity in MSC-*Luc2*. Cells were incubated with 1:1 D-luciferin (300µg/ml) and imaged on the IVIS Lumina II, according to the *in vitro* BLI acquisition settings. The image represented is at t= 30min after the addition of D-luciferin. Lane 1: D-PBS, Lane 2-10: MSC-*Luc2* and MSC-*Luc2/LacZ* (control); (c) Linear regression analysis of luminescent signal was performed using GraphPad Prism 7®. Data are presented as means ± SDs of triplicates.

We chose to assess the persistence of MSCs transplanted subcutaneously in immune-competent NOD and immune-deficient NOD/*Scid* animal models as this most closely reflects the route of administration of a cell replacement therapy for individuals with T1D. Thus, MSC-*Luc2* were transplanted subcutaneously at multiple cell concentrations to determine the lowest cell concentration and the length of time for which bioluminescence could be detected (**Fig. 3a**). Quantitative analysis of BLI data showed that in both NOD/*Scid* and NOD mice, there was an increase in bioluminescence with increasing cell dose (**Fig. 3b**), which resulted in a dose-dependent increase in persistence of bioluminescence in both animal models (**Supplementary Table 2a & 2b**). Bioluminescence, albeit diminished, could be detected in NOD/*Scid* mice for up to 12 weeks, suggesting poor survival of MSCs at the s.c transplant site. By comparison, bioluminescence persisted for 2 weeks in NOD mice, after which signal could no longer be detected, suggesting an immune-mediated clearing of the MSC graft. In fact, upon challenge with a follow-up injection of $1x10^6$ MSCs, clearing of the MSC graft occurred within 1 week post-injection (data not shown). These kinetics are consistent with the generation of memory T cell populations stimulated after the initial exposure to MSCs.

Neurod1 **and** ***Pdx1*** **fail to induce β-cell differentiation of** ***ex vivo*** **expanded NOD MSCs**

The pancreatic transcription factors, *Neurod1* and *Pdx1*, were over-expressed in MSC-*Luc2* to function as mediators of pancreatic transdifferentiation, whilst the *INS-FUR* gene was over-expressed to allow for mature human insulin production. Transduced MSCs were analysed via FACS and sorted into individual populations, as outlined in **Supplementary Table 3a & 3b**. The sorted MSCs were returned to culture and imaged for eGFP and mCherry expression 7 days post-transduction (**Fig. 4a & 4b**). As can be seen, eGFP expression in MSCs transduced with *Neurod1* and *INS-FUR/Neurod1* was lower than in cells transduced with the existing HMD and HMD-*INS-FUR* lentiviral vectors, a consequence of lower viral titers.

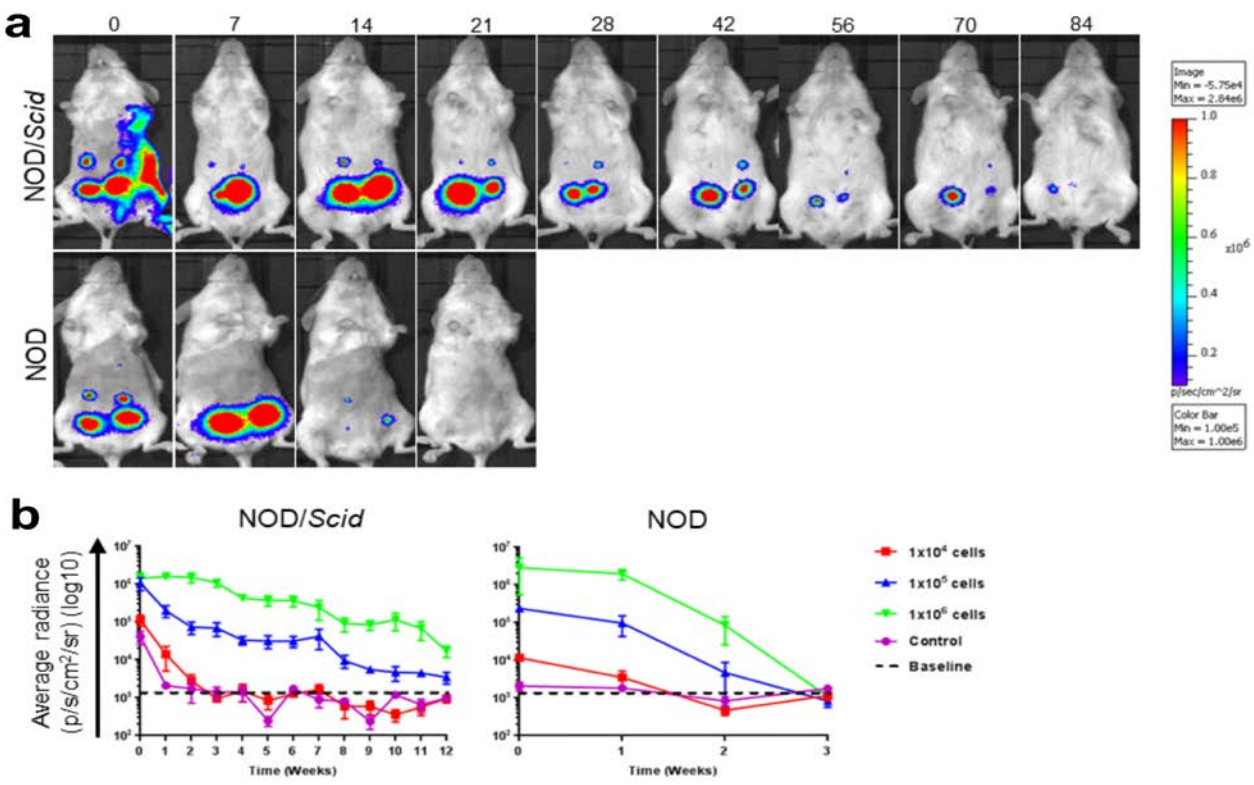

Figure 3: Persistence of syngeneic MSCs in immune-competent and immune-deficient animal models (a) NOD (n=4) and NOD/*Scid* (n=4) mice (6-10 weeks of age), received a total of six subcutaneous (s.c.) injections of $1x10^4$ (n=2), $1x10^5$ (n=2) and $1x10^6$ (n=2) mid-passage MSC-*Luc2* cells/mouse. Untreated age-matched NOD (n=2) and NOD/*Scid* (n=2) mice were utilized as negative controls. BLI images were acquired following i.p. administration of D-luciferin (15mg/mL) at 150mg/kg or 10µL/g. Images are representative of a single experimental NOD/*Scid* and NOD animal. (b) Analysis of MSC BLI in NOD and NOD/*Scid* mice. Regions of interest were established surrounding the areas corresponding to the sites of cell transplantation using the Living Image 3.1 (PerkinElmer™) software. Quantitative data was subsequently analyzed using GraphPad Prism 7®. Data were presented as mean radiance ± SEM over time (weeks). A two-way ANOVA and Tukey's post tests were performed, * $p<0.05$.

Transduced MSCs were subsequently cultured for a period of 28 days, at which point morphological analysis of the differentiation process was performed (**Fig. 4c**). Transduced MSCs expressing both murine *Neurod1* and *Pdx1* alone, or in combination with *INS-FUR*, retained a fibroblast-like morphology in comparison to their untransduced counterparts, demonstrating that no change in morphology was attributable to transgene over-expression.

Gene expression profiling was performed to determine if ectopic expression of *Neurod1*, *Pdx1* and *INS-FUR* in *ex vivo* expanded MSCs resulted in pancreatic differentiation. As can be seen in **Fig. 4d**, exogenous murine *Neurod1* was detected at 28 days post-transduction in MSCs transduced with HMD-*Neurod1* and

HMD-*INS-FUR/Neurod1*, and, as expected, expression was not detected in the parental MSCs, MSCs transduced with HMD and HMD-*INS-FUR*, and the positive control (mouse pancreas). Interestingly, exogenous *Neurod1* expression resulted in the expression of endogenous *Neurod1*, suggesting a potential auto-regulatory function of *Neurod1*. However, *Pdx1*, *Nkx6.1*, *Scl2a2*, *Ins1* and *Ins2* were not detected in parental and transduced MSCs. In **Fig. 4e**, a similar pattern of gene expression was observed following the ectopic expression of murine *Pdx1*, as was observed with ectopic expression of *Neurod1*, with the exception that ectopic *Pdx1* did not result in endogenous *Pdx1* expression. Together, these data confirm the lack of pancreatic differentiation in *ex vivo* expanded MSC expressing *Neurod1* and *Pdx1*.

Gene-modified *ex vivo* expanded NOD MSCs demonstrate abnormal glucose stimulated insulin secretion

The ability of transduced MSCs to secrete mature insulin *in vitro* in response to glucose stimulation was determined. A significant quantity of mature insulin (~4.5pmol/ml/1x10^5 cells) was detected in the medium of MSCs expressing *INS-FUR* alone, and in combination with *Pdx1*. By comparison, untransduced MSCs, and MSCs transduced with empty vector or *Neurod1* alone, did not secrete mature insulin (**Fig. 4f**). There was also a significant difference ($p<0.005$) in the quantity of insulin secreted between MSC-*INS-FUR* (~4.5pmol/ml/1x10^5 cells) and MSC-*INS-FUR/Neurod1* (~0.3pmol/ml/1x10^5 cells), which directly correlated with differences in the expression of the fluorescent reporter. Acute glucose stimulation assays showed that following stimulation with 20mM D-Glucose, glucose-stimulated insulin secretion (GSIS) was not present (**Fig. 4g**). The absence of GSIS was expected due to the lack of *Slc2a2* expression, as detected by RT-PCR.

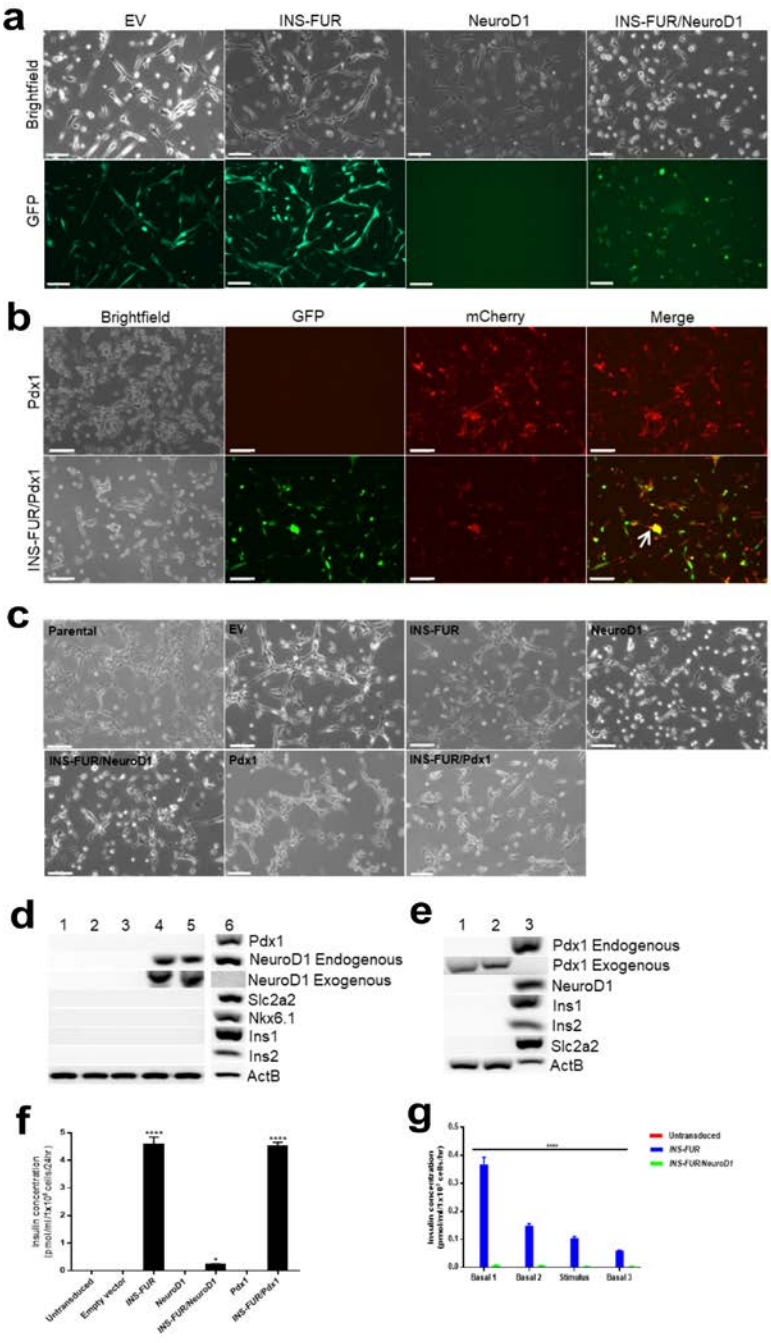

Figure 4: Analysis of *INS-FUR*, *Neurod1* and *Pdx1* transduced MSC (a) Fluorescence imaging of MSCs transduced with empty vector (EV), *Neurod1* and *INS-FUR*. Transduced cells were returned to culture after sorting for GFP positivity, and imaged for GFP expression (day 7 post-transduction) using a Leica DM fluorescence microscope (Leica Microsystems), 10x magnification with bright field and GFP fluorescence filter sets; scale bar = 100µm. (b) Fluorescence imaging of MSCs and MSC-*INS-FUR* transduced with *Pdx1*. Transduced cells were returned to culture post-sorting and imaged for GFP and mCherry expression (Day 7 post transduction) using a Leica DM microscope, 10x magnification under bright field, GFP and Texas Red fluorescence filter sets; scale bar =100µm. (c) Morphological characterization of MSCs post-transduction. Bright field images were acquired at 28 days post-transduction on a Leica DM microscope (Leica Microsystems) at 10x magnification under bright field setting; scale bar = 100µm. (d) Gene expression profiling of *INS-FUR* and *Neurod1*-expressing MSC. Lane 1: Untransduced MSC, Lane 2: MSC-*EV*, Lane 3: MSC-*INS-FUR*, Lane 4: MSC-*Neurod1*, Lane 5: MSC-*INS-FUR/Neurod1* and Lane 6: Mouse pancreas (positive control). (e) Gene expression profiling of *Pdx1*-expressing MSCs. Lane 1: MSC-*Pdx1*, Lane 2: MSC-*INS-FUR/Pdx1* and Lane 3: Mouse pancreas (positive control). (f) Chronic insulin secretion from transduced MSCs. Human insulin was quantified using the ARCHITECT™ i4000SR Immunoassay Analyser (Abbott Diagnostics©). Data are represented as means ± SDs (n=4). A one-way ANOVA with Sidak's post tests were performed, * p<0.05. (g) Acute glucose-stimulated insulin secretion from *INS-FUR* and *Neurod1* transduced MSCs. Human insulin was quantified using the ARCHITECT™ i4000SR Immunoassay Analyser (Abbott Diagnostics©). Data were presented as means ± SDs (n=3). Two-way ANOVAs with Tukey's post tests were performed, * p<0.05.

388 ***INS-FUR*-expressing MSCs fail to restore normoglycaemia in STZ-diabetic NOD/*Scid* mice**

389 To determine if *INS-FUR*-expressing MSCs could restore normoglycaemia in STZ-diabetic NOD/*Scid* mice,
390 animals received a s.c. transplant of either $1x10^7$ or $5x10^7$ cells. In animals treated with $5x10^7$ cells, within
391 24-hrs following transplantation there was a decrease in blood glucose concentrations; and a significant
392 ($p<0.05$) decrease was observed at days 8 and 12 post-transplantation (**Fig. 5a**). In addition, there was a
393 significant decrease in the blood glucose levels of the animals treated with $5x10^7$ cells, from before to
394 after transplantation, for a period of ~15 days (pre-transplant vs post-transplant, $p<0.05$) (**Supplementary**
395 **Table 4a & 4b**). By comparison, blood glucose concentrations in diabetic animals, and animals treated
396 with $1x10^7$ cells, remained significantly higher ($p<0.0001$) than the normal controls for the duration of the
397 experiment. Most importantly, animals treated with either $1x10^7$ or $5x10^7$ cells did not normalize blood
398 glucose concentration at any time for the duration of the experiment. In addition, there was a significant
399 difference in the body weights of treated animals in comparison to normal controls both before and after
400 transplantation, despite random allocation of animals to the different groups (**Fig. 5b**). However, at no
401 time-point was there a significant decrease in body weight observed over the time course of the
402 experiment.

403 Prior to euthanasia, animals treated with $5x10^7$ cells (n=3) were assessed for glucose tolerance via an
404 IPGTT. Treated animals displayed an abnormal glucose tolerance in comparison to normal controls (**Fig.**
405 **5c**). The high degree of variation in the glucose tolerance observed for the treatment group was due to
406 one treated animal beginning the IPGTT at a significantly lower blood glucose concentration than the
407 other treated animals, a consequence of the cell transplant having successfully reduced blood glucose
408 levels in this animal.

409

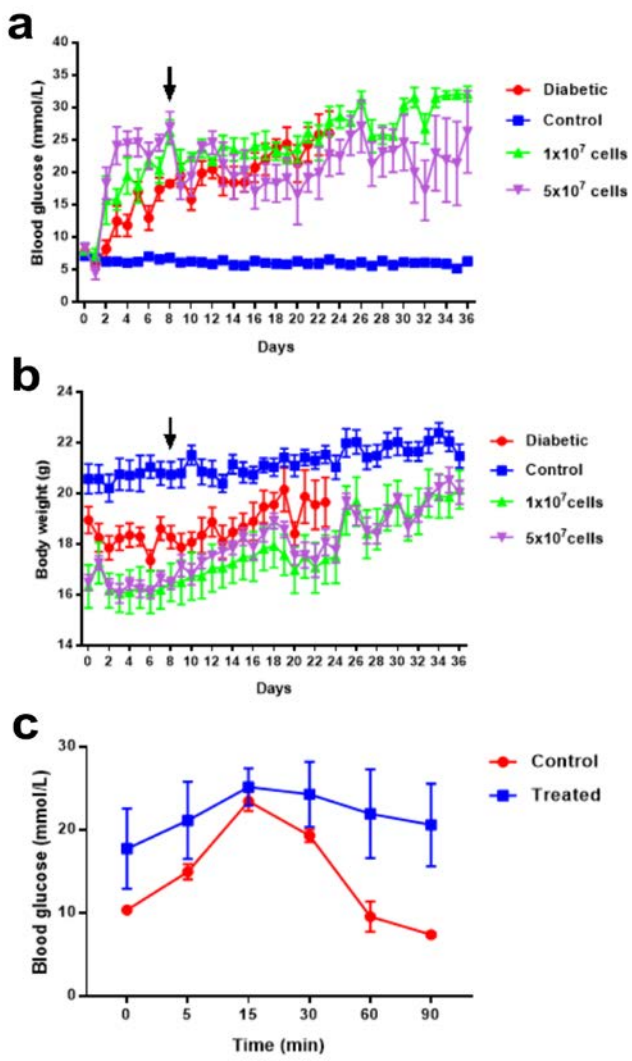

Figure 5: Transplantation of MSC-*INS-FUR* in STZ-diabetic NOD/*Scid* mice (a) Blood glucose concentrations of treated STZ-diabetic NOD/*Scid* mice. Blood glucose measurements were recorded daily post STZ-injection for the duration of the experiment (36 days). Data were presented as means ± SEMs (n=6 mice per group). Two-way ANOVAs with Sidak's post tests were performed, * $p<0.05$. (b) Body weights of treated STZ-NOD/*Scid* mice. Body weight measurements were recorded daily post STZ-injection for the duration of the experiment (36 days). Data were presented as means ± SEMs (n=6 mice per group). Two-way ANOVAs were performed with Sidak's post-tests, * $p<0.05$. (c) IPGTT in treated STZ-diabetic NOD/*Scid* mice. Blood glucose measurements were obtained at 0, 5, 15, 30, 60 and 90 min post D-glucose injection. Data were presented as means ± SEMs (n=5; normal, n=3; treated). Two-way ANOVAs with Sidak's post tests were performed, * $p<0.05$.

Discussion

Stem cells are characterized by two defining long-term characteristics; (i) the ability for renewal without differentiation into other cell types when cultured under standard conditions, and (ii) the continued potential to develop into specialized cell types when cultured under defined experimental conditions. The early, mid- and late-passage number NOD derived MSCs utilized in this study fulfilled the ISCT criteria of plastic adherence, self-renewal and colony formation without differentiation into other cell types under standard MSC culture conditions; and tri-lineage mesenchymal differentiation into bone, fat and cartilage under defined cell culture conditions[20, 21].

In this study, NOD derived MSCs maintained a fibroblast-like morphology, potent self-renewal and clonogenicity throughout early, mid and late passage numbers. This finding is in contrast to previous studies, which suggest that MSCs undergo age-related changes with continued cell passage[26-28]. The maintenance of a fibroblast-like morphology can be attributed, in part, to medium supplementation with bFGF. These results are supported by another study, where bFGF inhibited apoptosis and promoted proliferation of MSCs through a reduction in cellular oxidative stress[29]. Although MSC characteristics of self-renewal and colony forming units (CFU-F) were conserved following cell culture expansion, MSCs showed some reduction in tri-lineage differentiation with increasing passage, which is in concordance with other studies[30-32]. Furthermore, several studies have demonstrated the detrimental effect of aging on multipotential differentiation, proliferation and senescence[31, 33, 34]. Collectively, these findings highlight the importance of ongoing surveillance of stem cell-like properties, amongst other defining characteristics, when engineering replacement cell therapies.

To clarify whether NOD derived MSCs were immune-evasive, we subcutaneously transplanted syngeneic MSCs into immune-competent NOD mice, which were detectable by BLI up to 14 days post-transplantation. In a similar study, MSCs that were transduced to co-express luciferase and GFP, and subsequently transplanted via the kidney artery in BALB/c mice, were detected via BLI up to 14 days post transplantation[35]. This demonstrates that the site of cell administration in immune-competent models does not affect cell survival, and that syngeneic MSCs do not appear to be immune-privileged[36]. This may be due to several factors, including the over-expression of the non-mammalian *Luc2* transgene and contaminating FBS, factors that may override the inherent immune privilege characteristics of MSCs. In fact, previous studies have demonstrated that sustained high levels of luciferase expression induce luciferase-specific immune responses in immune-competent animal models, thereby limiting the utility of luciferase as an *in vivo* reporter in transplantation studies[37, 38].

However, in immune-deficient NOD/*Scid* mice, syngeneic MSCs were detected for a significantly longer period (up to 12 weeks post-transplantation), albeit with diminishing persistence. These results are supported by similar studies, which show loss of transplanted MSCs in immune-deficient animal models[39-41]. The current study highlights the importance of reporter gene selection, and the limited timeframe in which MSC therapeutic effects can be evaluated, in both immune-competent and immune-deficient animal models. Assessment of MSCs in short-term studies has demonstrated their protective benefits[42], whereas long-term studies show little or no protection[43], which may be attributable to their lack of persistence in immune-competent models.

We also assessed the ability to differentiate *ex vivo* expanded MSCs into surrogate β-cells. Considering the success of *Neurod1* as a mediator of β-cell differentiation in non-pancreatic tissues, we sought to determine the potential of *Neurod1* to induce β-cell differentiation of MSCs. In transduced MSCs, over-expression of *Neurod1* and *INS-FUR* did not result in the cuboidal morphological changes associated with β-cell differentiation. In addition, gene expression profiling confirmed a lack of β-cell differentiation due to the absence of expression of endogenous pancreatic transcription factors and insulin. A recent study by Qing-Song et al, assessed the effect of *Pdx1*, *Neurod1* and *MafA* over-expression in MSCs and showed that *Neurod1* was a weak inducer of endogenous *Pdx1* and *Ins2* expression, and that only in combination with *Pdx1* and *MafA* was there significant induction of β-cell differentiation and insulin expression[44]. Surprisingly, in this study, the lack of β-cell differentiation following over-expression of *Pdx1* in culture-expanded MSCs indicated that *ex vivo* expansion results in defects in the pancreatic differentiation potential of MSCs.

A previous study showed that *in vivo* transplantation is required for functional β-cell maturation[45], therefore *INS-FUR*-expressing MSCs were assessed for their ability to reverse diabetes following transplantation into STZ-diabetic NOD/*Scid* mice. Upon transplantation of $5x10^7$ *INS-FUR*-expressing

MSCs, blood glucose concentrations decreased from 25-30 to 15-20mmol/L. However, at no time point did blood glucose levels fall within the normal physiological range (5-7mmol/L). This is likely due to the severe hyperglycaemia induced in these animals, which likely requires higher cell numbers to restore blood glucose levels to within the normal physiological range. Despite this, there was a significant decrease in the blood glucose levels of treated vs diabetic animals ($p<0.05$), that was maintained for ~2 weeks, after which blood glucose concentrations began to increase to pre-transplant values. The subsequent increase in blood glucose concentrations of treated animals correlated with the results of the MSC persistence studies in NOD/*Scid* mice. In addition, IPGTTs of transplanted animals showed that they exhibited abnormal glucose tolerance, indicating a lack of *in vivo* GSIS. This finding corroborated the *in vitro* characterization studies.

In conclusion, the results of this study highlight several caveats to MSC-based gene therapy for T1D, which warrant careful consideration prior to the formulation of clinical trials. Considering that over-expression of *Pdx1* in early-passage MSCs results in pancreatic differentiation[14], these data show that *ex vivo* expansion impairs pancreatic differentiation of NOD derived MSCs through the age-related loss of multipotency. Therefore, gene modification should be performed as soon as practicable after the isolation of MSCs[46]. In addition, given that *ex vivo* expansion is required to generate sufficient quantities of adult derived MSCs for therapeutic purposes, and that this process impairs their therapeutic potential, the use of embryonic stem cells or induced pluripotent stem cells as an unlimited stem cell source may overcome this limitation[47, 48].

Data availability

The datasets used and/or analyzed during the current study are available from the corresponding author upon request.

Conflicts of interest

The authors declare that there are no conflicts of interest that could be perceived as prejudicing the impartiality of the research reported.

Funding

Research was supported by project grants from the Diabetes Australia Research Trust (DART) and the Rebecca L. Cooper Medical Research Foundation. An Australian Postgraduate Award and a scholarship from the Arrow Bone Marrow Transplant Foundation supported DG. RH was supported by a UTS Research Excellence PhD Scholarship and UTS Top-up Scholarship from the Translational Cancer Research Network (TCRN).

Author contributions

DG: conception and design, collection and presentation of data, data analysis and interpretation, manuscript writing; RMW: conception and design, DG and RMW performed MSC isolations, RMW performed MSC nucleofection, data analysis and interpretation, manuscript writing, and final approval of manuscript. RH performed chondrogenesis assays. BR, NTN and BOB contributed to the study design, data analysis and interpretation. AMS: financial support, conception and design, data analysis and interpretation, manuscript writing and final approval of manuscript. All authors read and approved the final manuscript.

Acknowledgements

Frank Kao and Steven Allen (Advanced Cytometry Facility, Centenary Institute, Sydney, Australia) for their assistance with FACS sorting. Fiona Ryan and Lalit Overlunde for animal husbandry and assistance with animal health monitoring (University of Technology Sydney, Australia).

References

1. Atkinson MA, Maclaren NK. The Pathogenesis of Insulin-Dependent Diabetes Mellitus. *The New England Journal of Medicine* 1994; **19**(331)**:** 1428-1436.

2. Meloche MR. Transplantation for treatment of type 1 diabetes. *World Journal of Gastroenterology* 2007; (13)**:** 6347-6355.

3. Ren B, O'Brien BA, Swan MA, Koina ME, Nassif N, Wei MQ *et al.* Long-term correction of diabetes in rats after lentiviral hepatic insulin gene therapy. *Diabetologia* 2007; **50**(9)**:** 1910-1920.

4. Ren B, O'Brien BA, Byrne MR, Ch'ng E, Gatt PN, Swan MA *et al.* Long-term reversal of diabetes in non-obese diabetic mice by liver-directed gene therapy. *J Gene Med* 2013; **15**(1)**:** 28-41.

5. Gerace D, Ren B, Hawthorne WJ, Byrne MR, Phillips PM, O'Brien BA *et al.* Pancreatic Transdifferentiation in Porcine Liver Following Lentiviral Delivery of Human Furin–Cleavable Insulin. *Transplantation Proceedings* 2013; **45**(5)**:** 1869-1874.

6. Xie Q-P, Huang H, Xu B, Dong X, Gao S-L, Zhang B *et al.* Human bone marrow mesenchymal stem cells differentiate into insulin-producing cells upon microenvironmental manipulation in vitro. *Differentiation* 2009; **77**(5)**:** 483-491.

7. Pagliuca FW, Millman JR, Gurtler M, Segel M, Van Dervort A, Ryu JH *et al.* Generation of functional human pancreatic beta cells in vitro. *Cell* 2014; **159**(2)**:** 428-439.

8. Oh S-H, Muzzonigro TM, Bae S-H, LaPlante JM, Hatch HM, Petersen BE. Adult bone marrow-derived cells trans-differentiating into insulin-producing cells for the treatment of type I diabetes. *Laboratory Investigation* 2004; **84**(5)**:** 607-617.

9. Tang DQ, Cao LZ, Burkhardt BR, Xia CQ, Litherland SA, Atkinson MA *et al.* In vivo and in vitro characterization of insulin-producing cells obtained from murine bone marrow. *Diabetes* 2004; **53**(7)**:** 1721-1732.

10. Wu XH, Liu CP, Xu KF, Mao XD, Zhu J, Jiang JJ *et al.* Reversal of hyperglycemia in diabetic rats by portal vein transplantation of islet-like cells generated from bone marrow mesenchymal stem cells. *World J Gastroenterol* 2007; **13**(24)**:** 3342-3349.

11. Chakrabarti SK, Mirmira RG. Transcription factors direct the development and function of pancreatic beta cells. *TRENDS in Endocrinology and Metabolism* 2003; **14**(2)**:** 78-84.

12. Gerace D, Martiniello-Wilks R, O'Brien BA, Simpson AM. The use of β-cell transcription factors in engineering artificial β-cells from non-pancreatic tissue. *Gene Ther* 2015; **22**(1)**:** 1-8.

13. Kojima H, Fujimiya M, Matsumura K, Younan P, Imaeda H, Maeda M *et al.* NeuroD-betacellulin gene therapy induces islet neogenesis in the liver and reverses diabetes in mice. *Nat Med* 2003; **9**(5)**:** 596-603.

14. Karnieli O, Izhar-Prato Y, Bulvik S, Efrat S. Generation of insulin-producing cells from human bone marrow mesenchymal stem cells by genetic manipulation. *STEM CELLS* 2007; **25**(11)**:** 2837-2844.

15. Li Y, Zhang R, Qiao H, Zhang H, Wang Y, Yuan H *et al.* Generation of insulin-producing cells from PDX-1 gene-modified human mesenchymal stem cells. *Journal of Cellular Physiology* 2007; **211**(1)**:** 36-44.

16. Lin G, Wang G, Liu G, Yang LJ, Chang LJ, Lue TF *et al.* Treatment of type 1 diabetes with adipose tissue-derived stem cells expressing pancreatic duodenal homeobox 1. *Stem Cells Dev* 2009; **18**(10)**:** 1399-1406.

17. Kajiyama H, Hamazaki TS, Tokuhara M, Masui S, Okabayashi K, Ohnuma K *et al.* Pdx1-transfected adipose tissue-derived stem cells differentiate into insulin-producing cells in vivo and reduce hyperglycemia in diabetic mice. *Int J Dev Biol* 2010; **54**(4)**:** 699-705.

18. Ren B, Tao C, Swan MA, Joachim N, Martiniello-Wilks R, Nassif NT *et al.* Pancreatic Transdifferentiation and Glucose-Regulated Production of Human Insulin in the H4IIE Rat Liver Cell Line. *International Journal of Molecular Sciences* 2016; **17**(4)**:** 534.

19. Dodson BP, Levine AD. Challenges in the translation and commercialization of cell therapies. *BMC Biotechnology* 2015; **15**(1)**:** 70.

20. Dominici M, Le Blanc K, Mueller I, Slaper-Cortenbach I, Marini F, Krause D *et al.* Minimal criteria for defining multipotent mesenchymal stromal cells. The International Society for Cellular Therapy position statement. *Cytotherapy* 2006; **8**(4)**:** 315-317.

21. Galipeau J, Krampera M, Barrett J, Dazzi F, Deans RJ, DeBruijn J *et al.* International Society for Cellular Therapy perspective on immune functional assays for mesenchymal stromal cells as potency release criterion for advanced phase clinical trials. *Cytotherapy* 2016; **18**(2)**:** 151-159.

22. Ferber S, Halkin A, Cohen H, Ber I, Einav Y, Goldberg I *et al.* Pancreatic and duodenal homeobox gene 1 induces expression of insulin genes in liver and ameliorates streptozotocin-induced hyperglycemia. *Nat Med* 2000; **6**(5)**:** 568-572.

23. Council NHaMR. *Australian code for the care and use of animals for scientific purposes*, 2013.

24. Wang HS, Hung SC, Peng ST, Huang CC, Wei HM, Guo YJ *et al.* Mesenchymal stem cells in the Wharton's jelly of the human umbilical cord. *Stem Cells* 2004; **22**(7)**:** 1330-1337.

25. Lawandi J, Tao C, Ren B, Williams P, Ling D, Swan MA *et al.* Reversal of diabetes following transplantation of an insulin-secreting human liver cell line: Melligen cells. *Molecular Therapy — Methods & Clinical Development* 2015; **2:** 15011.

26. Bonab MM, Alimoghaddam K, Talebian F, Ghaffari SH, Ghavamzadeh A, Nikbin B. Aging of mesenchymal stem cell in vitro. *BMC Cell Biology* 2006; **7**(1)**:** 14.

27. Peffers MJ, Collins J, Fang Y, Goljanek-Whysall K, Rushton M, Loughlin J *et al.* Age-related changes in mesenchymal stem cells identified using a multi-omics approach. *European cells & materials* 2016; **31:** 136-159.

28. Stolzing A, Jones E, McGonagle D, Scutt A. Age-related changes in human bone marrow-derived mesenchymal stem cells: consequences for cell therapies. *Mechanisms of ageing and development* 2008; **129**(3)**:** 163-173.

29. Nawrocka D, Kornicka K, Szydlarska J, Marycz K. Basic Fibroblast Growth Factor Inhibits Apoptosis and Promotes Proliferation of Adipose-Derived Mesenchymal Stromal Cells Isolated from Patients with Type 2 Diabetes by Reducing Cellular Oxidative Stress. *Oxidative Medicine and Cellular Longevity* 2017; **2017:** 22.

30. Yu JM, Wu X, Gimble JM, Guan X, Freitas MA, Bunnell BA. Age-related changes in mesenchymal stem cells derived from rhesus macaque bone marrow. *Aging cell* 2011; **10**(1)**:** 66-79.

31. Marędziak M, Marycz K, Tomaszewski KA, Kornicka K, Henry BM. The Influence of Aging on the Regenerative Potential of Human Adipose Derived Mesenchymal Stem Cells. *Stem Cells International* 2016; **2016:** 2152435.

32. Kretlow JD, Jin Y-Q, Liu W, Zhang WJ, Hong T-H, Zhou G *et al.* Donor age and cell passage affects differentiation potential of murine bone marrow-derived stem cells. *BMC Cell Biology* 2008; **9**(1)**:** 60. doi: 10.1186/1471-2121-9-60

33. Kornicka K, Marycz K, Tomaszewski KA, Maredziak M, Smieszek A. The Effect of Age on Osteogenic and Adipogenic Differentiation Potential of Human Adipose Derived Stromal Stem Cells (hASCs) and the Impact of Stress Factors in the Course of the Differentiation Process. *Oxidative Medicine and Cellular Longevity* 2015; **2015:** 20.

34. Zhang D, Lu H, Chen Z, Wang Y, Lin J, Xu S *et al.* High glucose induces the aging of mesenchymal stem cells via Akt/mTOR signaling. *Molecular medicine reports* 2017; **16**(2)**:** 1685-1690.

35. Bai ZM, Deng XD, Li JD, Li DH, Cao H, Liu ZX *et al.* Arterially transplanted mesenchymal stem cells in a mouse reversible unilateral ureteral obstruction model: in vivo bioluminescence imaging and effects on renal fibrosis. *Chinese medical journal* 2013; **126**(10)**:** 1890-1894.

36. Ankrum JA, Ong JF, Karp JM. Mesenchymal stem cells: immune evasive, not immune privileged. *Nature biotechnology* 2014; **32**(3)**:** 252-260.

37. Podetz-Pedersen KM, Vezys V, Somia NV, Russell SJ, McIvor RS. Cellular immune response against firefly luciferase after sleeping beauty-mediated gene transfer in vivo. *Human gene therapy* 2014; **25**(11)**:** 955-965.

618 38. Yin Y, Takahashi Y, Hamana A, Nishikawa M, Takakura Y. Effects of transgene expression level per
619 cell in mice livers on induction of transgene-specific immune responses after hydrodynamic gene
620 transfer. *Gene Ther* 2016; **23**(7)**:** 565-571.

621 39. Rosova I, Dao M, Capoccia B, Link D, Nolta JA. Hypoxic preconditioning results in increased motility
622 and improved therapeutic potential of human mesenchymal stem cells. *Stem Cells* 2008; **26**(8)**:**
623 2173-2182.

624 40. Meyerrose TE, De Ugarte DA, Hofling AA, Herrbrich PE, Cordonnier TD, Shultz LD *et al.* In vivo
625 distribution of human adipose-derived mesenchymal stem cells in novel xenotransplantation
626 models. *Stem Cells* 2007; **25**(1)**:** 220-227.

627 41. Meyerrose TE, Roberts M, Ohlemiller KK, Vogler CA, Wirthlin L, Nolta JA *et al.* Lentiviral-
628 transduced human mesenchymal stem cells persistently express therapeutic levels of enzyme in
629 a xenotransplantation model of human disease. *Stem Cells* 2008; **26**(7)**:** 1713-1722.

630 42. Choi EW, Shin IS, Park SY, Yoon EJ, Kang SK, Ra JC *et al.* Characteristics of mouse adipose tissue-
631 derived stem cells and therapeutic comparisons between syngeneic and allogeneic adipose tissue-
632 derived stem cell transplantation in experimental autoimmune thyroiditis. *Cell transplantation*
633 2014; **23**(7)**:** 873-887.

634 43. Liang J, Li X, Zhang H, Wang D, Feng X, Wang H *et al.* Allogeneic mesenchymal stem cells
635 transplantation in patients with refractory RA. *Clinical rheumatology* 2012; **31**(1)**:** 157-161.

636 44. Qing-Song G, Ming-Yan Z, Lei W, Xiang-Jun F, Yu-Hua L, Zhi-Wei W *et al.* Combined Transfection
637 of the Three Transcriptional Factors, PDX-1, NeuroD1, and MafA, Causes Differentiation of Bone
638 Marrow Mesenchymal Stem Cells into Insulin-Producing Cells. *Experimental Diabetes Research*
639 2012; **2012:** 10.

45. D'Amour KA, Bang AG, Eliazer S, Kelly OG, Agulnick AD, Smart NG *et al.* Production of pancreatic hormone-expressing endocrine cells from human embryonic stem cells. *Nat Biotechnol* 2006; **24**(11)**:** 1392-1401.

46. Gerace D, Martiniello-Wilks R, Nassif NT, Lal S, Steptoe R, Simpson AM. CRISPR-targeted genome editing of mesenchymal stem cell-derived therapies for type 1 diabetes: a path to clinical success? *Stem Cell Research & Therapy* 2017; **8**(1)**:** 62.

47. Frith JE, Thomson B, Genever PG. Dynamic three-dimensional culture methods enhance mesenchymal stem cell properties and increase therapeutic potential. *Tissue engineering. Part C, Methods* 2010; **16**(4)**:** 735-749.

48. Karlsson C, Emanuelsson K, Wessberg F, Kajic K, Axell MZ, Eriksson PS *et al.* Human embryonic stem cell-derived mesenchymal progenitors—Potential in regenerative medicine. *Stem Cell Research* 2009; **3**(1)**:** 39-50.